

# VibCReg: Variance-Invariance-better-Covariance Regularization for Self-Supervised Learning on Time Series

Daesoo Lee<sup>1</sup> and Erlend Aune<sup>1,2</sup>

<sup>1</sup>Norwegian University of Science and Technology

<sup>2</sup>BI Norwegian Business School

## Abstract

Self-supervised learning for image representations has recently had many breakthroughs with respect to linear evaluation and fine-tuning evaluation. These approaches rely on both cleverly crafted loss functions and training setups to avoid the feature collapse problem. In this paper, we improve on the recently proposed VICReg paper, which introduced a loss function that does not rely on specialized training loops to converge to useful representations. Our method improves on a *covariance* term proposed in VICReg, and in addition we augment the head of the architecture by an IterNorm layer that greatly accelerates convergence of the model. Our model achieves superior performance on linear evaluation and fine-tuning evaluation on a subset of the UCR time series classification archive and the PTB-XL ECG dataset.

Source code will be made available.

## 1 Introduction

In the last year, representation learning (RL) has had great success within computer vision, improving both on SOTA for fine-tuned models and achieving close-to SOTA results on linear evaluation on the learned representations [1, 2, 3, 4, 5, 6, 7], and many more. The main idea in these papers is to train a high-capacity neural network using a self-supervised learning (SSL) loss that is able to produce representations of images that are useful for downstream tasks such as image classification and segmentation. The recent mainstream SSL frameworks can be divided into two main categories: 1) contrastive learning method, 2) non-contrastive learning method. The representative contrastive learning methods such as MoCo [3] and SimCLR [8] use positive and negative pairs and they learn representations by pulling the representations of the positive pairs together and pushing those of the negative pairs apart. However, these methods require a large number of negative pairs per positive pair to learn representations effectively. To eliminate a need for negative pairs, a non-contrastive learning method such as BYOL [4], SimSiam [5], Barlow Twins [6], and VICReg [7] have been proposed. Since the non-contrastive learning methods use positive pairs only, their architectures could be simplified. The non-contrastive learning methods were also able to outperform the existing contrastive learning methods.

To further improve quality of learned representations, feature whitening and feature decorrelation have been a main idea behind some recent improvements [9, 6, 10, 7]. Initial SSL frameworks such as SimCLR suffered from a problem called feature collapse if there are not enough negative pairs, where the collapsing denotes that features of the representations collapse to constants. The collapsing occurs since a similarity metric is still high even if all the features converged to constants, which is the reason for the use of the negative pairs to prevent the collapsing. The collapsing has been partially resolved by using a momentum encoder [4], an asymmetric framework with a predictor, and stop-gradient [4, 5], which have popularized the non-contrastive learning methods. However, one of the latest SSL frameworks, VICReg, shows

that none of them is needed and it is possible to conduct effective representation learning with the simplest Siamese architecture without the collapsing via the feature decorrelation. Using this idea for SSL has first shown up in W-MSE [9] in a recent year where the feature components are decorrelated from each other by whitening. Later, Barlow Twins encodes the feature decorrelation by reducing off-diagonal terms of its cross-correlation matrix to zero. Hua et al. [10] encodes the feature decorrelation by introducing Decorrelated Batch Normalization (DBN) [11] and Shuffled-DBN. VICReg encodes the feature decorrelation by introducing variance and covariance regularization terms in its loss function in addition to a similarity loss.

The mainstream SSL frameworks have been developed in a computer vision domain, and the SSL for time series problems has seen much less attention despite its evident abundance in industrial, financial, and societal applications. The Makridakis competitions [12, 13] give examples of important econometric forecasting challenges. The UCR Archive [14] is a collection of datasets where classification is of importance, and in the industrial setting, sensor data and Internet of Things (IoT) data are examples where proper machine learning tools for time series modeling is important. Publicly-available ECG datasets such as CinC [15] and PTB-XL [16] consist of 12-lead ECG signal data and data labels are heart disease diagnoses. Thus, classification is of importance for the ECG datasets.

In this paper, we investigate several existing mainstream SSL frameworks on several time series datasets, and propose a SSL framework, VIBCReg (Variance-Invariance-better-Covariance Regularization), which is inspired by the feature decorrelation methods from [9, 10, 7] and it can be viewed an upgraded version of VICReg by having the better covariance regularization. The existing SSL frameworks investigated in this paper are CPC, SimSiam, Barlow Twins, and VICReg. In addition, we also investigated incorporation of VIBCReg with a recent work, Mean Shift (MSF) [17], in an attempt to optimize the invariance term in a better way. Mean Shift is an extended version of BYOL by pulling one view to its  $k$ -neighbors instead of one-to-one pulling. All the frameworks are reproduced and the source code will be made available.

Since the mainstream SSL frameworks from computer vision have been developed focused on a classification task, we investigate SSL frameworks on a time series classification task. In this paper, we investigate the performance of VIBCReg and its competitors on the following datasets: 1) the ten datasets of the UCR archive with the highest number of time series within them, 2) the five datasets of the UCR archive with the highest number of labels, where a dataset has more than 900 samples, 3) the PTB-XL.

One recent study regarding SSL on 12-lead ECG datasets [18] has investigated SSL frameworks such as SimCLR, BYOL, SwAV [19], and a modified CPC on 12-lead ECG datasets. SSL is conducted on a combination of several publicly-available 12-lead ECG datasets and evaluated by linear evaluation and fine-tuning evaluation. It showed that the modified CPC proposed by the authors perform the best. However, the modifications made on the original CPC by removing strides in the convolutional layers, therefore, its architecture is not generic and not suitable for general time series. Also, a large portion of performance gain of the modified CPC is not from its architecture but from a two-step fine-tuning technique where a classification head is first trained with an encoder frozen for the first  $n$  epochs, and the classification head and the encoder are both trained after  $n$  epochs. Although our paper addresses SSL on a 12-lead ECG dataset, the main focus differs from [18] in a sense that our focus lies on comparative performances of SSL frameworks on time series data while Mehari and Strodthoff [18] focuses on the highest possible classification performance on the ECG dataset by utilizing SSL.

In the following sections, related works and the proposed methods are introduced, and experimental results are followed. An overview of comparative linear evaluation results on the UCR datasets are presented in Fig. 1.

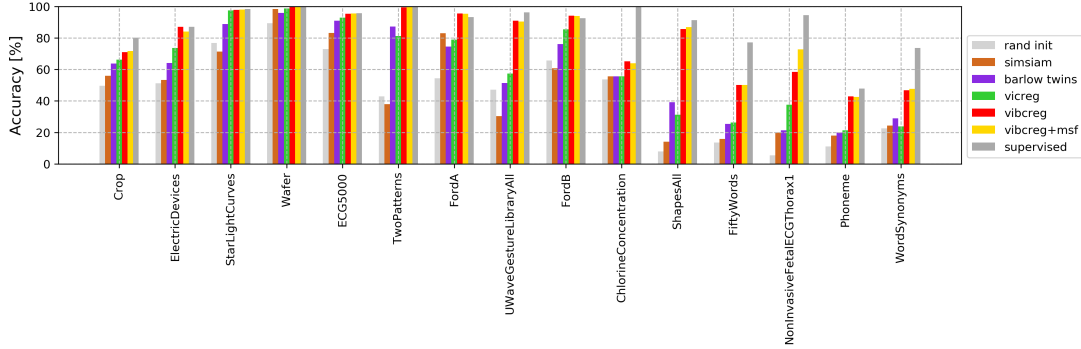


Figure 1: Comparative linear evaluation results on the UCR datasets. **rand init** denotes using a randomly-initialized frozen encoder and **supervised** denotes an encoder trained in a supervised-learning manner. **vibcreg+msf** denotes VbCReg+Mean Shift (MSF). It is shown that VbCReg(+MSF) not only outperforms all the other frameworks, but also it even outperforms **supervised** on some datasets. Note that VbCReg+MSF is termed VbCReg.

## 2 Related Works

### 2.1 Contrastive Learning Methods

#### 2.1.1 Siamese Architecture-based SSL Frameworks

A framework of a Siamese neural network [21] is illustrated in Fig. 2. The Siamese neural network has two branches with a shared encoder on each side, and its similarity metric is computed based on two representations from the two encoders. Its main purpose is to learn representations such that two representations are similar if two input images belong to the same class and two representations are dissimilar if two input images belong to the different classes. One of the main applications of the Siamese neural network is one-shot and few-shot learning for image verification [21, 20] where a representation of a given image can be obtained by an encoder of a trained Siamese neural network and it is compared with representations of the existing images for the verification by a similarity metric. It should be noted that the Siamese neural network is trained in a supervised manner with a labeled dataset. The learning process of the representations by training an encoder is termed representation learning.

Although representation learning can be conducted using the Siamese neural network, its capability is somewhat limited by the fact that it utilizes supervised learning where a labeled dataset is required. To eliminate a need for a labeled dataset and still be able to conduct effective representation learning, SSL has become very popular where unlabeled datasets are utilized to train an encoder. Some of the representative contrastive learning methods that are based on the Siamese architecture are MoCo and SimCLR. Both frameworks are illustrated in Fig. 2.

**MoCo** The contrastive learning methods require a large number of negative pairs per positive pair, and MoCo keeps a large number of negative pairs by having a queue where a current mini-batch of representations is enqueued and the oldest mini-batch of representations in the queue is dequeued. A similarity loss is computed using representations from the encoder and the momentum encoder, and the dissimilarity loss is computed using representations from the encoder and the queue, and they are merged to form a form of a contrastive loss function, called InfoNCE [22]. The momentum encoder is a moving average of the encoder and it maintains consistency of the representations.

**SimCLR** It greatly simplifies a framework for the contrastive learning. Its major components are 1) a projector after a ResNet backbone encoder [23], 2) InfoNCE based on a large mini-batch. The projector is a small neural network that maps representations to the space where contrastive loss is applied. By having this, quality of representations could be improved

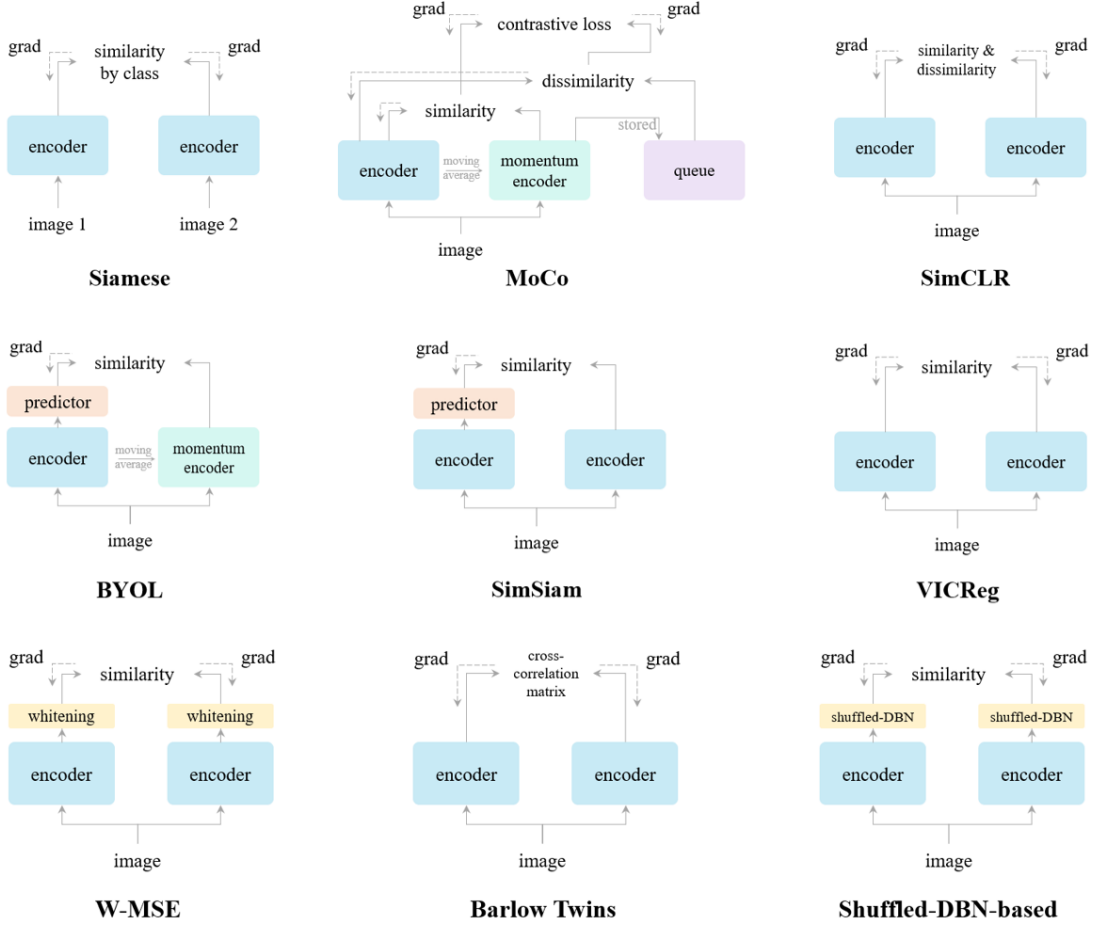


Figure 2: Comparison on Siamese architecture-based SSL frameworks. Siamese denotes the Siamese architecture [20] and the others are SSL frameworks. The encoder includes all layers that can be shared between both branches. The dash lines indicate the gradient propagation flow. Therefore, the lack of a dash line denotes stop-gradient.

by leaving the downstream task to the projector while the encoder is trained to output better quality representations.

### 2.1.2 Contrastive Predictive Coding

**CPC** It is quite different from those Siamese-based frameworks in a sense that its key insight is to learn useful representations by predicting the future in latent space by using an autoregressive model. CPC uses a convolutional neural network (CNN)-based encoder and a GRU-based autoregressive model [24]. The encoder compresses high-dimensional data into a much more compact latent embedding space in which conditional predictions are easier to model, and the autoregressive model makes predictions many steps in the future after processing representations encoded by the encoder.

## 2.2 Non-Contrastive Learning Methods

The representative non-contrastive learning methods are BYOL and SimSiam. Both frameworks are illustrated in Fig. 2.

**BYOL** It has gained a great popularity by proposing a framework that does not require any negative pair for the first time. Before BYOL, a large mini-batch size was required [8] or

some kind of memory bank [25, 3] was needed to keep a large number of negative pairs. Grill et al. [4] hypothesized that BYOL may avoid the collapsing without a negative pair due to a combination of 1) addition of a predictor to an encoder, forming an asymmetrical architecture and 2) use of the momentum encoder.

**SimSiam** It can be viewed as a simplified version of BYOL by removing the momentum encoder. Chen and He [5] empirically showed that a stop-gradient is critical to prevent the collapsing.

### 2.2.1 Feature Decorrelation Considered

The frameworks that improved the representation learning using the idea of the feature decorrelation are W-MSE, Barlow Twins, and a Shuffled-DBN-based framework. They are illustrated in Fig. 2.

**W-MSE** Its core idea is to whiten feature components of representations so that the feature components are decorrelated from each other, which can eliminate feature redundancy. The whitening process used in W-MSE is based on a Cholesky decomposition [26] proposed by Siarohin et al. [27].

**Barlow Twins** It encodes a similarity loss (invariance term) and a loss for feature decorrelation (redundancy reduction term) into the cross-correlation matrix. The cross-correlation is computed by conducting matrix multiplication of  $z_i^T z_j$  where  $z_i \in \mathbb{R}^{B \times F}$  and  $z_j \in \mathbb{R}^{B \times F}$  and  $B$  and  $F$  denote batch size and feature size, respectively. Then, representation learning is conducted by optimizing the cross-correlation matrix to be an identity matrix, where optimization of the diagonal terms corresponds to that of a similarity loss and optimization of the off-diagonal terms corresponds to that of the feature decorrelation loss.

**DBN-based framework** Its authors Hua et al. [10] categorized the feature collapsing into two categories: 1) *complete collapse*, caused by constant feature components, 2) *dimensional collapse*, caused by redundant feature components. They pointed out that previous works had mentioned and addressed the complete collapse only but not the dimensional collapse. Its main idea is to use DBN to normalize the output from its encoder-projector, which provides the feature decorrelation effect, and the feature decorrelation prevents the dimensional collapse. To further decorrelate the features, Shuffled-DBN is proposed, in which an order of feature components is randomly arranged before DBN and the output is rearranged back to the original feature-wise order.

### 2.2.2 Feature Decorrelation and Feature-component Expressiveness Considered

**VICReg** VICReg encodes *Feature Decorrelation* (FD) and *Feature-component Expressiveness* (FcE) in its loss function in addition to a similarity loss, where FD and FcE are termed *variance term* and *covariance term* in the VICReg paper, respectively. A high FcE indicates that output values from a feature component have a high variance and vice versa. Hence, a (near)-zero FcE indicates the complete collapse. Its strength lies in its simplicity such that VICReg uses the simplest Siamese form and does not require either the stop-gradient, asymmetrical architecture, or whitening/normalization layer. Despite its simplicity, its performance is very competitive compared to other latest SSL frameworks.

## 2.3 No-striding CPC

Mehari and Strodthoff [18] uses a no-striding CPC, a modified version of the original CPC by removing strides in the convolutional layers. Its performance on the ECG datasets was verified to be better than that of SimCLR, BYOL, and SwAV, which is somewhat surprising given the fact that SimCLR, BYOL, and SwAV outperform CPC with an apparent margin in computer vision [7]. This indicates that CPC is competitively effective compared to SimCLR, BYOL, and SwAV at learning representations of time series data. However, since the no-striding CPC does not use any stride, one feature component in a representation is mapped over a very-short length in the original space of data. Therefore, the no-striding CPC is not generic for processing general

time series. Specifically, it is not suitable when long chunks of time series need to be processed. Since SimCLR, BYOL, and SwAV are already investigated on the 12-lead ECG dataset in [18], we decided to investigate more recent SSL frameworks than SimCLR, BYOL, and SwAV such as SimSiam, Barlow Twins, and VICReg under an assumption that the more recent SSL frameworks should perform better than previous ones since the more recent frameworks are algorithmically improved versions of the previous ones. Also, the original implementation of CPC is investigated to put a focus on comparative performances of SSL frameworks to find out which framework has a higher potential for robust time series representation learning.

It should be noted that evaluation of CPC is conducted only on the PTB-XL since its input window length is already suggested (*i.e.*, 2.5s) [18]. Since CPC’s input window length depends on architectural properties (*i.e.*, number of striding convolutional layers and striding size), architecture of the CPC’s encoder would need to be changed for every UCR dataset. Also, CPC wouldn’t even possible to be used on datasets with short length such as Crop since it needs time series that is long enough for the multiple step predictions.

## 2.4 Mean Shift

Mean Shift (MSF) is a recent SSL framework, and it can be viewed as an extended version of BYOL. In BYOL, two positive views are pulled to optimize the invariance term (*i.e.*, similarity loss). MSF improved it by pulling one view to its  $k$ -neighbors, where the neighbors are fetched from a memory bank. By having this better invariance term, MSF could outperform BYOL. We adopted MSF into our VlbCReg to derive the better invariance.

## 3 Proposed Method

VlbCReg (Variance-Invariance-better-Covariance Regularization) is inspired by and concurrent with a recent SSL framework, VICReg (Variance-Invariance-Covariance Regularization), and it can be viewed as VICReg with a better covariance regularization. It should be noted that the variance, invariance, and covariance terms in VICReg correspond to what we call the *feature component expressiveness* (FcE), similarity loss, and *feature decorrelation* (FD) terms in VlbCReg, respectively. By having the better covariance regularization, VlbCReg could outperform VICReg in terms of the learning speed, linear evaluation, and semi-supervised training. What motivated VlbCReg are the followings: 1) FD has been one of the key components for improvement of quality of learned representations [9, 6, 11, 7], 2) Hua et al. [10] showed that application of DBN and Shuffled-DBN on the output from an encoder-projector is very effective for faster and further FD, 3) addressing FcE in addition to FD is shown to be effective [7], 4) scale of the VICReg’s FD loss (covariance term) varies depending on feature size and its scale range is quite wide due to its summation over the covariance matrix. Hence, we assumed that a scale of the VICReg’s FD loss could be modified to be consistent and to have a small range so that a weight parameter for the FD loss would not have to be re-tuned in accordance with a change of the feature size.

VlbCReg is illustrated in Fig. 3 in comparison to VICReg. In Fig. 3,  $t$  and  $t'$  are sampled from a distribution  $T$  to produce two different views of each input data. The views are encoded using the encoder into representations  $Y$  and  $Y'$ . The representations are further processed by the projector and an iterative normalization (IterNorm) layer [28] into projections  $Z$  and  $Z'$ . The loss is computed at the projection level on  $Z$  and  $Z'$ .

We describe here a loss function of VlbCReg, which consists of a similarity loss, FcE loss, and FD loss. It should be noted that the similarity loss and the FcE loss are defined the same as in VICReg. The input data is processed in batches, and we denote  $Z = [z_1, \dots, z_B]^T \in \mathbb{R}^{B \times F}$  and  $Z' = [z'_1, \dots, z'_B]^T \in \mathbb{R}^{B \times F}$  where  $B$  and  $F$  denote batch size and feature size, respectively. The *similarity loss* (*invariance term*) is defined as Eq. (1). The *FcE loss* (*variance term*) is defined as Eq. (2), where  $\text{Var}(\cdot)$  denotes a variance estimator,  $\gamma$  is a target value for the standard deviation, fixed to 1 in our experiments,  $\epsilon$  is a small scalar (*i.e.*, 0.0001) preventing numerical instabilities.

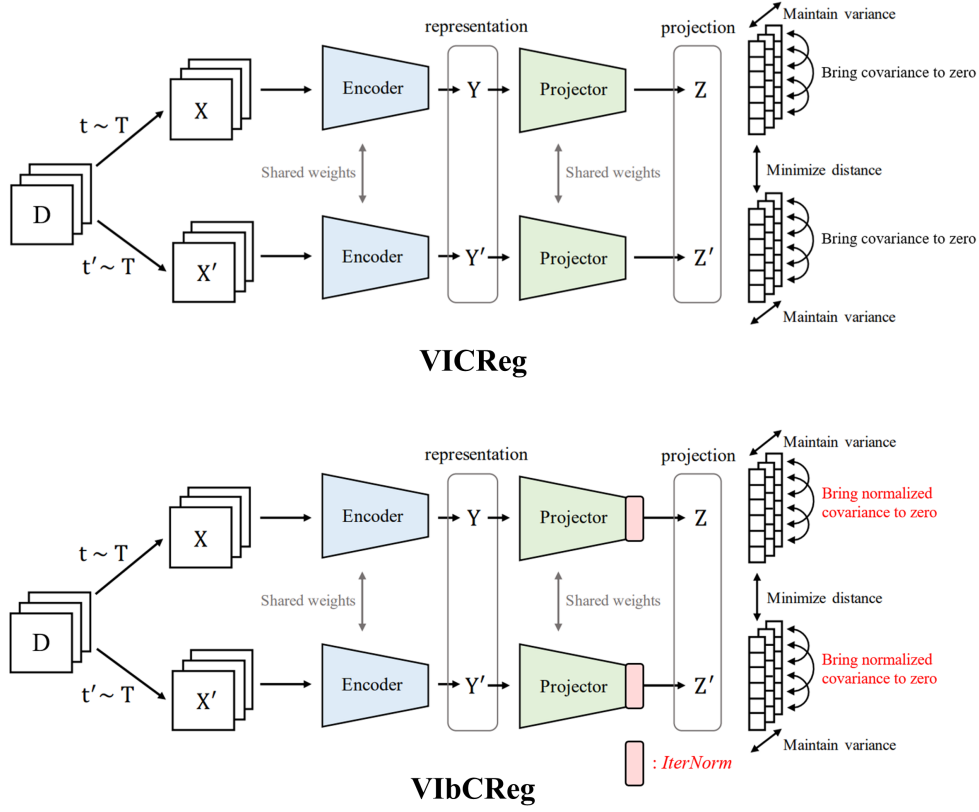


Figure 3: Comparison between VICReg and VIBCReg, where the difference is highlighted in red. As for VIBCReg, given a batch of input data  $D$ , two batches of different views  $X$  and  $X'$  are produced and are then encoded into representations  $Y$  and  $Y'$ . The representations are further processed into projections  $Z$  and  $Z'$  via the projector and an iterative normalization (IterNorm) layer. Then, the similarity between  $Z$  and  $Z'$  is maximized, the variance along the batch dimension is maximized, while the feature components of  $Z$  and  $Z'$  are progressively being decorrelated from each other, respectively.

$$s(Z, Z') = \frac{1}{B} \sum_{b=1}^B \|Z_b - Z'_b\|_2^2 \quad (1)$$

$$v(Z) = \frac{1}{F} \sum_{f=1}^F \text{ReLU} \left( \gamma - \sqrt{\text{Var}(Z_f) + \epsilon} \right) \quad (2)$$

The *FD loss* is the only component of VIBCReg's loss that differs from the corresponding *covariance term* in the loss of VICReg, thus, we here present a comparison between the two. The covariance matrix of  $Z$  in VICReg is defined as Eq. (3), and the covariance matrix in VIBCReg is defined as Eq. (4) where the  $\ell_2$ -norm is conducted along the batch dimension. Then, the FD loss of VICReg is defined as Eq. (5) and that of VIBCReg is defined as Eq. (6). Eq. (4) constrains the terms to range from -1 to 1, and Eq. (6) takes a mean of the covariance matrix by dividing the summation by a number of the matrix elements. Hence, Eq. (4) and Eq. (6) keep a scale and a range of the FD loss neat and small.

$$C(Z)_{\text{VICReg}} = \frac{1}{B-1} (Z - \bar{Z})^T (Z - \bar{Z}) \quad \text{where } \bar{Z} = \frac{1}{B} \sum_{b=1}^B Z_b \quad (3)$$

$$C(Z)_{\text{VibCReg}} = \left( \frac{Z - \bar{Z}}{\|Z - \bar{Z}\|_2} \right)^T \left( \frac{Z - \bar{Z}}{\|Z - \bar{Z}\|_2} \right) \quad (4)$$

$$c(Z)_{\text{VICReg}} = \frac{1}{F} \sum_{i \neq j} C_{\text{VICReg}}(Z)_{i,j}^2 \quad (5)$$

$$c(Z)_{\text{VibCReg}} = \frac{1}{F^2} \sum_{i \neq j} C_{\text{VibCReg}}(Z)_{i,j}^2 \quad (6)$$

The overall loss function is a weighted average of the similarity loss, FcE loss, and FD loss:

$$l(Z, Z') = \lambda s(Z, Z') + \mu \{v(Z) + v(Z')\} + \nu \{c(Z) + c(Z')\} \quad (7)$$

where  $\lambda$ ,  $\mu$ , and  $\nu$  are hyper-parameters controlling the importance of each term in the loss. In our experiments,  $\lambda$  and  $\mu$  are set to 25 and 25, respectively, following the VICReg paper.  $\nu$  for VICReg is set to 1 as in the VICReg paper, and  $\nu$  for VibCReg is empirically set to 200. Yet, it should be noted that the performance of VibCReg is quite consistent with respect to a choice of the weight parameter for  $\nu$  thanks to the use of the normalized covariance, Eq. (4).

Another key component in VibCReg is *IterNorm*. [10] showed that applying DBN on the output from an encoder-projector could improve representation learning, emphasizing that the whitening process helps the learning process, which corresponds to a main argument in the DBN paper [11]. To further improve DBN, IterNorm was proposed [28]. IterNorm was verified to be more efficient at the whitening than DBN by employing Newton’s iteration to approximate a whitening matrix. Therefore, we employ IterNorm instead of DBN, and IterNorm is applied to the output from an encoder-projector as shown in Fig. 3. Then, feature decorrelation is strongly supported, induced by the following two factors: 1) IterNorm, 2) optimization of the FD loss. IterNorm has two hyperparameters of an iteration number and group size. They are set to 5 and 64, respectively, as recommended in the IterNorm paper [10]. A pseudocode for VibCReg is presented in Appendix A.

**Relation to VICReg** To summarize, VibCReg can be viewed as VICReg with the normalized covariance matrix (instead of the covariance matrix) and IterNorm.

**VibCReg+MSF (VbIbCReg)** We also investigate the incorporation of VibCReg with MSF, which is proposed to derive the better invariance term. Hence, it is termed *VbIbCReg* (Variance-better-Invariance-better-Covariance Regularization) The incorporation is fairly simple: VibCReg’s similarity loss is changed to Eq. (8), where  $\ell_2$ -norm is along the feature dimension. For VICReg and VibCReg, MSE loss results in better representation learning than applying  $\ell_2$ -norm on  $Z$  as shown in [7]. However, optimization of the invariance term is conducted in the normalized embedding space for MSF [17]. Therefore, to mitigate between the two, we adopt the hybrid similarity loss function as Eq. (8). Finally, a loss function of VibCReg+MSF is defined as Eq.(9), where  $s_{\text{msf}}$  denotes the MSF’s similarity loss and  $\xi$  its weight hyperparameter. Note that  $s_{\text{msf}}$  is computed by similarity between one sample and its  $k$ -neighbors, where the neighbors are fetched from a memory bank. In our experiments,  $\xi$  is set to 5 to slightly add the MSF’s effect onto VibCReg. MSF has three hyperparameters: 1) memory bank size, 2) a number of neighbors  $k$ , 3) momentum of a target encoder. The memory bank size is set such that the size can roughly cover an entire training dataset, and  $k$  is set to 2 since  $k=2$  is shown to be effective enough in the MSF paper and our training datasets are relatively much smaller than ImageNet. The momentum of a target encoder is set to 0.99 as in the MSF paper. The architectural details of VbIbCReg are specified in Appendix B.

$$s'(Z, Z') = s(Z, Z')/2 + s\left(\frac{Z}{\|Z\|_2}, \frac{Z'}{\|Z'\|_2}\right)/2 \quad (8)$$

$$l(Z, Z') = \lambda s'(Z, Z') + \mu \{v(Z) + v(Z')\} + \nu \{c(Z) + c(Z')\} + \xi s_{\text{msf}} \quad (9)$$



## 4 Experimental Evaluation

**Datasets** In our experiments, two datasets are used: 1) the UCR archive, from which we select the 10 largest datasets together with the 5 datasets with more than 900 samples having the largest number of classes, and 2) the PTB-XL (12-lead ECG dataset). For the UCR datasets, each dataset is split into 80% (training set) and 20% (test set) by a stratified split. A model pre-training by SSL is conducted and evaluated on each dataset. Therefore, the UCR datasets are independent of one another in our experiments. The PTB-XL dataset comes with 71 labels and its evaluation task is framed as a multi-label classification task. The dataset is organized into ten stratified, label-balanced folds, where the first eight are used as a training set, the ninth is used as a validation set, and the tenth fold is used as a test set. As for the preprocessing, the UCR datasets are preprocessed by z-normalization followed by arcsinh, and the PTB-XL does not need any preprocessing since it is provided, preprocessed. Summaries of the UCR datasets and the PTB-XL are presented in Table 1 and Table 2, respectively.

Dataset name	#Samples	#Classes	Length
Crop	24000	24	46
ElectricDevices	16637	7	96
StarLightCurves	9236	3	1024
Wafer	7164	2	152
ECG5000	5000	5	140
TwoPatterns	5000	4	128
FordA	4921	2	500
UWaveGestureLibraryAll	4478	8	945
FordB	4446	2	500
ChlorineConcentration	4307	3	166
ShapesAll	1200	60	512
FiftyWords	905	50	270
NonInvasiveFetalECGThorax1	3765	42	750
Phoneme	2110	39	1024
WordSynonyms	905	25	270

Table 1: Summary of the UCR datasets. The first 10 datasets are the 10 largest datasets from the UCR archive, and the second 5 datasets are the datasets with the 5 largest number of classes from the UCR archive, where a dataset has more than 900 samples.

Dataset name	#Samples	#Classes	#Patients	Sampling frequency	Length
PTB-XL	21837	71	18885	100Hz	10s

Table 2: Summary of PTB-XL. Note that its step length is 1000 (*i.e.*, 10s  $\times$  100Hz).

**Training** For an optimizer, AdamW [29] ( $lr=0.001$ , weight decay=0.00001, batch size=256) is used with training epochs of 200. For a learning rate scheduler, a cosine learning rate decay is used [30]. Data augmentation methods used during the training are **Random Crop**, **Random Amplitude Resize**, and **Random Vertical Shift**. The details of the augmentation methods are presented in Appendix C. Note that the data augmentation is not used for CPC following the original implementation and the previous study [22, 18].

As for the deep learning library and the used GPU model, PyTorch [31] is used for building and training models with a single GPU (GTX1080-Ti).

## 4.1 Architecture

**Encoder** We follow the convention of the previous SSL papers by using ResNet [4, 5, 6, 7] for an encoder. But since the dataset size is much smaller than the size for SSL in computer vision, we use a *light-weighted* 1D ResNet, inspired by [32]. The detailed architecture is illustrated in Appendix D. It is used as an encoder for SimSiam, Barlow Twins, VICReg, VbCReg, and VbIbCReg.

**VbCReg** Its projector consists as follows: (Linear-BN-ReLU)-(Linear-BN-ReLU)-(Linear-IterNorm), where Linear, BN, and ReLU denotes a linear layer, batch normalization [33], and rectified linear unit, respectively. The dimension of the inner and output layers of the projector is set to 4096.

**Competing SSL Frameworks** The competing SSL frameworks are SimSiam, Barlow Twins, VICReg, and CPC. In our experiments, these competing frameworks are implemented as close as possible to the original implementations. The only major difference is the encoder’s dimension. Instead of 2-dimensional image input, they receive 1-dimensional time series input. Unless specified differently, the architectures follow original implementations.

**SimSiam** Except for the encoder, all the architectural settings are the same as in the original SimSiam paper [5].

**Barlow Twins** In the original implementation, the size of linear layers in the projector is set to 8192. In our experiments, the size is set to 4096. Barlow Twins has a hyperparameter of  $\lambda$ . It is set to  $5 \cdot 10^{-3}$  as in the original implementation.

**VICReg** In the original implementation, the size of linear layers in the projector is set to 8192. In our experiments, the size is set to 4096. Its hyperparameters of  $\lambda, \mu, \nu$  are set as in the original implementation (25, 25, and 1, respectively).

**CPC** It uses a downsampling CNN model as an encoder. In the original implementation, the CNN model consists of five convolutional layers with strides [5, 4, 2, 2, 2], filter-sizes [10, 8, 4, 4, 4], and 512 hidden units with ReLU activations. Then, there is a feature vector for every 10ms of speech on the 16KHz PCM audio waveform. Since time series data from the PTB-XL has relatively much lower sampling frequency (*i.e.*, 100Hz), the downsampling rate should be smaller. The CNN model in our experiments consists of four convolutional layers with strides [4, 3, 3, 2], filter-sizes [8, 6, 6, 4], and 512 hidden units with ReLU activations. Then, there is a feature vector for 1.96s on the 100Hz ECG time series data. Its maximum prediction step is set to 4.

## 4.2 Linear Evaluation

We follow the linear evaluation protocols from the computer vision domain [4, 5, 6, 7, 17]. Given the pre-trained encoder, we train a supervised linear classifier on the frozen features from the encoder. For the Siamese-based frameworks, the features are from the ResNet’s global average pooling (GAP) layer, and for CPC, the features are from its downsampling CNN model followed by a GAP layer. The linear classifier is trained with AdamW and ( $lr=0.001$ , batch size=256, weight decay=0.00001, training epochs=50). The learning rate gets reduced by the cosine learning rate decay. The used data augmentation methods are **Random Amplitude Resize** and **Random Vertical Shift**. Experimental results for the linear evaluation are presented in Table 3 and Table 4 on the UCR datasets and the PTB-XL, respectively.

Dataset Name	Rand Init	SimSiam	Barlow Twins	VICReg	VIbCReg	VbIbCReg	Supervised
Crop	49.6(0.1)	56.0(0.8)	63.7(0.7)	66.2(9.5)	<u>71.0(0.7)</u>	<b>71.7(0.3)</b>	80.1(0.4)
ElectricDevices	51.2(0.7)	53.2(4.3)	64.1(1.1)	73.6(0.1)	<b>87.1(0.3)</b>	<u>84.0(0.4)</u>	87.0(0.2)
StarLightCurves	76.7(2.3)	71.3(8.5)	88.7(4.2)	97.5(0.1)	<b>97.8(0.1)</b>	<b>97.9(0.1)</b>	98.3(0.1)
Wafer	89.4(0.0)	98.4(0.4)	95.9(0.4)	98.8(0.2)	<b>99.5(0.1)</b>	<b>99.6(0.1)</b>	99.9(0.0)
ECG5000	72.9(11.5)	83.1(5.5)	90.9(1.2)	92.8(0.0)	<b>95.4(0.1)</b>	<b>95.5(0.1)</b>	95.8(0.1)
TwoPatterns	42.8(1.6)	37.9(4.4)	87.2(6.5)	81.2(0.6)	<u>99.3(0.2)</u>	<b>99.6(0.2)</b>	100.0(0.0)
FordA	54.5(0.9)	83.0(4.1)	74.5(4.3)	79.0(0.3)	<b>95.5(0.3)</b>	<b>95.4(0.3)</b>	93.3(0.3)
UWaveGestureLibraryAll	47.2(1.3)	30.3(6.8)	51.3(5.6)	57.5(0.8)	<b>90.9(0.4)</b>	<u>90.4(0.3)</u>	96.2(0.4)
FordB	65.7(1.1)	60.8(5.4)	76.1(1.6)	85.4(0.3)	<b>94.0(0.3)</b>	<b>93.8(0.3)</b>	92.4(0.5)
ChlorineConcentration	53.6(0.0)	55.7(0.0)	55.5(0.3)	55.5(0.1)	<b>65.2(0.7)</b>	<u>64.0(0.8)</u>	100.0(0.0)
ShapesAll	<u>7.9(2.5)</u>	<u>14.1(3.1)</u>	<u>39.2(3.6)</u>	<u>31.2(2.4)</u>	<u>85.7(0.8)</u>	<b>86.9(1.0)</b>	91.2(1.0)
FiftyWords	13.6(1.7)	15.8(2.1)	25.4(1.7)	26.3(0.9)	<b>50.2(1.1)</b>	<b>50.1(0.8)</b>	77.2(1.2)
NonInvasiveFetalECGThorax1	5.0(0.8)	20.0(3.6)	21.4(8.8)	37.6(0.7)	<u>58.5(0.6)</u>	<b>72.8(0.6)</b>	94.5(0.3)
Phoneme	11.1(0.0)	18.1(0.6)	19.9(1.5)	21.4(0.2)	<b>42.8(0.5)</b>	<b>42.6(0.2)</b>	47.8(1.0)
WordSynonyms	22.1(0.9)	24.4(0.4)	29.0(1.3)	23.8(0.3)	<u>46.7(0.7)</u>	<b>47.6(0.8)</b>	73.7(1.8)

Table 3: Linear evaluation on the UCR datasets. The results are obtained over 5 runs with different random seeds for the stratified split. It is noticeable that the proposed frameworks outperform the other frameworks with significant margins, and they even outperform **Supervised** on some datasets. A major difference between VIbCReg and VbIbCReg can be found on the 5 datasets with the 5 highest number of classes (*i.e.*, from ShapesAll to WordSynonyms). The values within the parentheses are standard deviations. Note that **Rand Init** denotes a randomly-initialized frozen encoder with a linear classifier on the top and **Supervised** denotes a trainable encoder-linear classifier trained in a supervised manner.

PTB-XL	Rand Init	CPC	SimSiam	Barlow Twins	VICReg	VIbCReg	VbIbCReg	Supervised
Macro AUC	0.4634(137)	0.8268(20)	0.5899(356)	0.7524(224)	0.8316(11)	<b>0.8478(31)</b>	<u>0.8444(32)</u>	0.9311(18)
Valid. loss	0.1078(2)	0.0799(3)	0.1025(9)	0.0906(33)	0.0791(2)	<u>0.0750(2)</u>	<b>0.0747(2)</b>	0.0629(2)
Test loss	0.1071(2)	0.0806(1)	0.1013(10)	0.0890(26)	0.0788(3)	<u>0.0760(2)</u>	<b>0.0758(2)</b>	0.0612(3)

Table 4: Linear evaluation on the PTB-XL. The results are obtained over 5 runs. For the PTB-XL, a macro AUC score is commonly used as a linear evaluation score [34, 18]. Additionally, the lowest validation and test losses are presented to cover an aspect of the evaluation that the macro AUC cannot cover. The validation loss is computed on the 9-th fold in the same setting as the training, and the test loss is computed on the 10-th fold in the same setting as the training except that no augmentation is applied on input data. Note that a binary cross entropy loss for multiple classes is used (*i.e.*, `BCEWithLogitsLoss` in PyTorch). The standard deviation values within the parentheses are presented, multiplied by 10000 (*i.e.*, 0.0002  $\rightarrow$  2).

### 4.3 Fine-tuning Evaluation on a Small Dataset

Fine-tuning evaluation on a subset of training dataset is conducted to do the ablation study. We follow the ablation study protocols from the computer vision domain [4, 5, 6, 7, 17]. Given the pre-trained encoder, we fine-tune the pre-trained encoder and train the linear classifier. AdamW optimizer is used with ( $lr_{enc}$ =0.0001,  $lr_{cls}$ =0.001, batch size=256, weight decay=0.001, training epochs=100), where  $lr_{enc}$  and  $lr_{cls}$  denote learning rates for the encoder and the linear classifier, respectively. During the fine-tuning, the BN statistics are set such that they can be updated. The used data augmentation methods are **Random Amplitude Resize** and **Random Vertical Shift**. Experimental results for the fine-tuning evaluation on the UCR datasets and the PTB-XL are presented in Table 5 and Table 6, respectively.

Dataset name	SimSiam	Barlow Twins	VICReg	VlbCReg	VbIbCReg	Supervised
<i>Fine-tuning evaluation on 5% of the training dataset</i>						
Crop	61.6(0.6)	60.5(0.5)	61.6(2.4)	62.4(0.3)	<b>63.9(0.8)</b>	62.6(0.7)
ElectricDevices	71.4(2.8)	69.2(1.5)	73.1(0.3)	<b>84.7(0.4)</b>	82.7(0.2)	69.0(0.9)
StarLightCurves	85.3(0.1)	93.0(4.3)	<b>98.1(0.1)</b>	<b>98.1(0.1)</b>	<b>98.2(0.0)</b>	97.8(0.2)
Wafer	<b>99.3(0.1)</b>	98.8(0.1)	<b>99.4(0.1)</b>	99.1(0.2)	<b>99.3(0.1)</b>	<b>99.3(0.2)</b>
ECG5000	91.4(1.2)	91.8(0.8)	94.0(0.5)	94.1(0.6)	<b>94.3(0.4)</b>	94.1(0.4)
TwoPatterns	49.3(8.5)	96.2(2.2)	98.6(0.4)	<b>99.2(0.5)</b>	<b>99.4(0.2)</b>	88.0(4.2)
FordA	91.1(1.0)	80.6(3.5)	90.1(0.6)	<b>94.4(0.6)</b>	<b>94.3(0.4)</b>	89.8(1.0)
UWaveGestureLibraryAll	42.9(11.3)	55.1(4.6)	77.1(2.2)	<b>83.4(2.3)</b>	<b>83.7(1.5)</b>	78.5(1.1)
FordB	74.3(5.3)	82.4(2.1)	90.0(0.4)	<b>92.2(0.7)</b>	<b>92.3(0.8)</b>	87.4(1.9)
ChlorineConcentration	57.4(0.7)	55.9(0.5)	56.7(1.0)	61.7(1.7)	61.8(2.0)	<b>65.6(1.9)</b>
NonInvasiveFetalECGThorax1	33.4(2.5)	21.2(6.1)	44.2(2.6)	45.6(1.9)	55.9(1.9)	<b>66.9(3.8)</b>
<i>Fine-tuning evaluation on 10% of the training dataset</i>						
Crop	66.2(0.6)	65.3(0.4)	66.4(1.9)	66.3(0.4)	<b>68.0(0.6)</b>	67.0(0.7)
ElectricDevices	75.1(1.9)	73.8(0.8)	75.9(0.5)	<b>86.5(0.6)</b>	85.4(0.5)	73.4(0.7)
StarLightCurves	91.8(5.3)	97.4(0.3)	<b>98.2(0.1)</b>	<b>98.2(0.1)</b>	<b>98.2(0.0)</b>	98.0(0.2)
Wafer	<b>99.6(0.1)</b>	99.4(0.1)	<b>99.6(0.1)</b>	<b>99.5(0.1)</b>	<b>99.5(0.1)</b>	<b>99.6(0.1)</b>
ECG5000	93.2(0.3)	93.1(0.5)	94.6(0.7)	<b>95.0(0.5)</b>	<b>95.1(0.4)</b>	94.4(0.7)
TwoPatterns	93.0(5.0)	99.5(0.5)	99.7(0.1)	<b>99.9(0.1)</b>	<b>99.9(0.1)</b>	<b>99.9(0.1)</b>
FordA	92.4(0.1)	87.5(1.4)	92.8(0.3)	<b>94.8(0.2)</b>	<b>94.8(0.1)</b>	91.7(0.3)
UWaveGestureLibraryAll	58.1(14.0)	68.5(3.2)	84.9(1.0)	<b>91.2(1.2)</b>	<b>91.1(1.2)</b>	84.7(0.9)
FordB	89.3(0.6)	89.3(1.9)	91.3(0.6)	<b>93.0(0.5)</b>	92.5(0.3)	89.1(0.3)
ChlorineConcentration	63.4(0.7)	56.2(0.3)	60.6(1.3)	72.2(2.6)	71.5(2.3)	<b>76.7(2.2)</b>
ShapesAll	21.8(6.2)	35.4(3.4)	38.2(2.5)	67.8(3.1)	<b>68.4(2.2)</b>	50.2(4.0)
NonInvasiveFetalECGThorax1	38.1(5.6)	24.4(3.7)	45.7(1.9)	61.8(1.6)	70.3(2.4)	<b>77.4(4.1)</b>
WordSynonyms	29.3(1.1)	34.4(2.5)	40.3(1.4)	45.4(2.6)	<b>48.8(3.0)</b>	36.2(2.4)
<i>Fine-tuning evaluation on 20% of the training dataset</i>						
Crop	70.4(0.5)	70.2(0.4)	70.4(1.3)	70.6(0.5)	<b>71.8(0.2)</b>	71.1(0.6)
ElectricDevices	80.4(0.9)	79.7(0.5)	79.0(0.2)	<b>88.1(0.3)</b>	87.5(0.2)	78.5(0.6)
StarLightCurves	98.0(0.3)	98.0(0.2)	<b>98.4(0.1)</b>	<b>98.3(0.1)</b>	<b>98.3(0.0)</b>	98.2(0.1)
Wafer	<b>99.7(0.1)</b>	<b>99.6(0.1)</b>	<b>99.6(0.1)</b>	<b>99.6(0.1)</b>	<b>99.6(0.1)</b>	<b>99.7(0.1)</b>
ECG5000	94.3(0.7)	94.4(0.2)	95.3(0.2)	<b>95.6(0.3)</b>	<b>95.7(0.4)</b>	95.3(0.2)
TwoPatterns	<b>99.9(0.1)</b>	<b>99.9(0.2)</b>	<b>100.0(0.0)</b>	<b>100.0(0.0)</b>	<b>100.0(0.0)</b>	<b>100.0(0.0)</b>
FordA	93.2(0.5)	91.2(0.5)	93.2(0.4)	<b>95.0(0.4)</b>	<b>95.2(0.5)</b>	92.2(0.6)
UWaveGestureLibraryAll	78.0(8.6)	85.5(1.4)	89.2(0.4)	<b>94.5(0.7)</b>	94.1(0.6)	89.7(1.0)
FordB	91.0(0.5)	91.8(0.4)	92.1(0.5)	<b>93.7(0.5)</b>	93.4(0.4)	90.8(0.3)
ChlorineConcentration	85.4(1.1)	56.7(0.7)	81.4(0.9)	88.4(0.9)	88.7(1.1)	<b>93.2(1.1)</b>
ShapesAll	27.6(11.2)	48.8(3.5)	53.6(0.6)	79.6(1.9)	<b>80.2(2.5)</b>	66.6(3.6)
FiftyWords	31.7(1.3)	47.1(1.9)	46.7(2.7)	<b>56.4(1.7)</b>	<b>56.0(0.8)</b>	49.0(1.9)
NonInvasiveFetalECGThorax1	72.9(3.2)	49.8(2.1)	79.7(1.1)	83.0(0.8)	85.1(0.4)	<b>87.4(0.7)</b>
Phoneme	27.5(2.0)	27.8(1.0)	34.5(1.1)	<b>41.5(1.4)</b>	40.9(1.6)	32.8(1.6)
WordSynonyms	32.7(4.9)	42.4(2.7)	47.7(3.3)	<b>55.9(2.9)</b>	<b>55.9(1.9)</b>	47.8(3.2)

Table 5: Fine-tuning evaluation on subsets of the UCR datasets. The results are obtained over 5 runs with different random seed for the stratified split. In 5% and 10%, results on some datasets missing because the split training subsets are too small.

PTB-XL	CPC	SimSiam	Barlow Twins	VICReg	VlbCReg	VblbCReg	Supervised
Macro AUC	0.8313(30)	0.8179(120)	0.8325(39)	<b>0.8692(25)</b>	0.8514(26)	0.8506(27)	0.8643(12)
Valid. loss	0.0768(3)	0.0845(20)	0.0802(6)	0.0754(3)	0.0750(2)	<b>0.0743(1)</b>	0.0765(2)
Test loss	0.0776(3)	0.0831(14)	0.0792(11)	<b>0.0749(4)</b>	0.0764(2)	0.0757(2)	<b>0.0749(3)</b>

Table 6: Fine-tuning evaluation on a subset of the PTB-XL, where the subset used for the fine-tuning is the 1st fold. That is, 12.5% of the training dataset. The results are obtained over 5 runs.

#### 4.4 Faster Representation Learning by VlbCReg

On the top of the outstanding performance, VlbCReg has another strength: *faster representation learning*, which makes VlbCReg more appealing compared to its competitors. The speed of representation learning is presented by kNN classification accuracy for the UCR datasets [5] in Fig. 4 and by kNN macro F1 score [35] for the PTB-XL in Fig. 5 along with *FD metrics*  $\mathcal{M}_{\text{FD}}$  and *FcE metrics*  $\mathcal{M}_{\text{FcE}}$ . The FD metrics and FcE metrics are metrics for the feature decorrelation and feature component expressiveness. The low FD metrics indicates high feature decorrelation (*i.e.*, features are well decorrelated) and vice versa. The low FcE metrics indicates the feature collapse and vice versa. Note that VlbCReg and VblbCReg are trained to have the FcE metrics of 1. Details of both metrics are specified in Appendix E. To keep this section neat, the corresponding FD and FcE metrics of Figs. 4-5 are presented in Appendix F.1.

To provide further analysis with respect to the faster representation learning, linear evaluation results with the pretrained encoders of 10 epochs and 100 epochs on the UCR datasets are presented in Fig. 6.

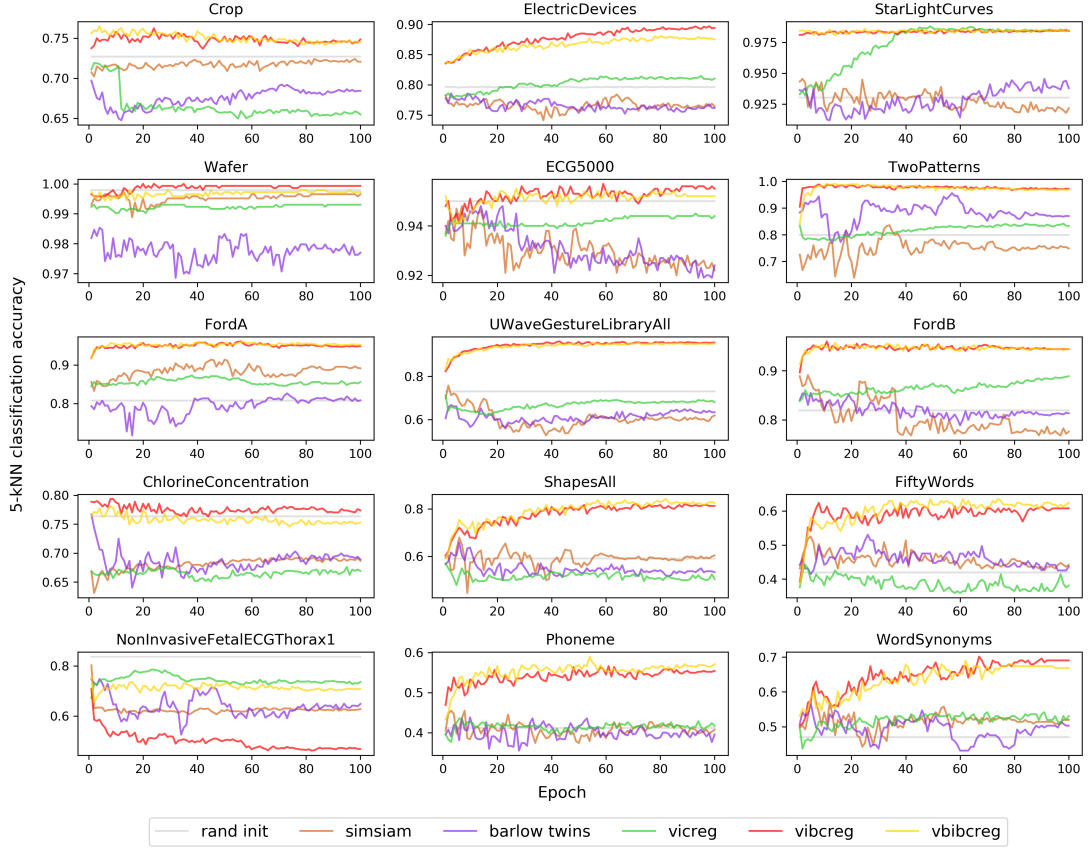


Figure 4: 5-kNN classification accuracy on the UCR datasets during the representation learning. It is recognizable that VIBCReg and VbIBCReg shows the fastest convergence and the highest kNN accuracy on most of the datasets.

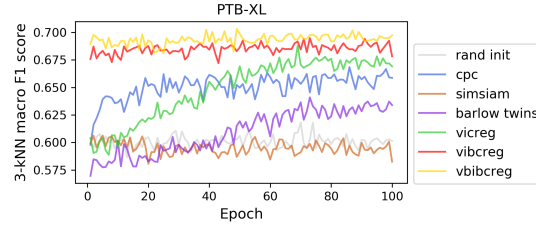


Figure 5: kNN macro F1 score on the PTB-XL dataset during the representation learning. Similar to the kNN accuracy on the UCR datasets, VIBCReg and VbIBCReg result in the higher kNN classification accuracy with the fastest convergence.

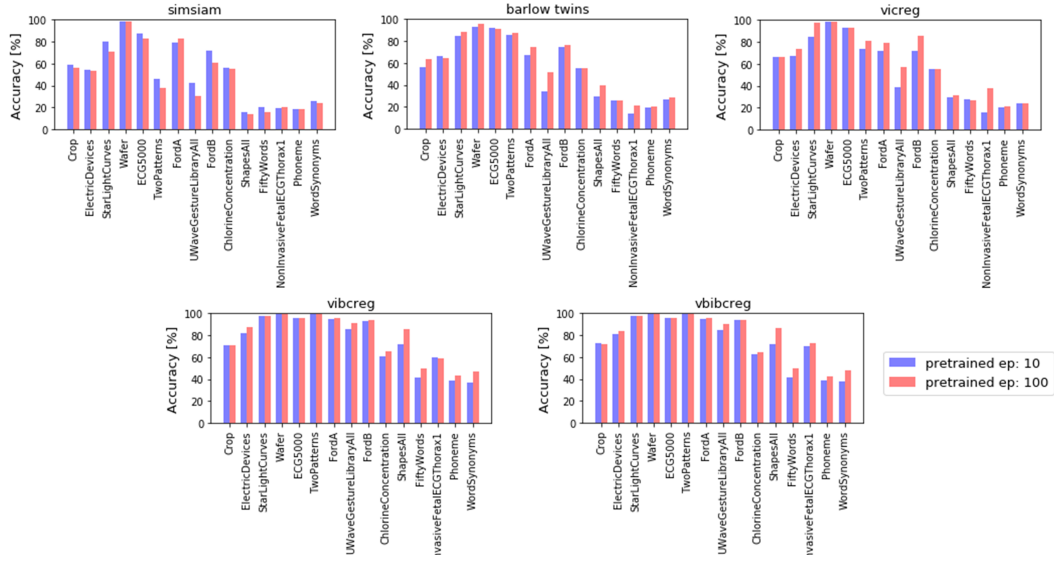


Figure 6: Linear evaluation results with the pretrained encoders of 10 epochs and 100 epochs on the UCR datasets. VbICReg and VbIBCReg shows much smaller gaps between **ep:10** and **ep:100** on many datasets. This fast learning can reduce a significant amount of computational cost for the pretraining.

#### 4.5 Between VICReg and VbICReg

As mentioned earlier in Section 3, VbICReg can be viewed as VICReg with the normalized covariance matrix (NCM) and IterNorm. In this section, frameworks between VICReg and VbICReg are investigated as shown in Table 7. The linear evaluation results of the four frameworks on the UCR datasets are presented in Fig. 7. The corresponding kNN accuracy graphs are also presented in Fig. 8 to show the learning progress, and the corresponding FD and FcE metrics graphs are presented in Appendix F.2.

Frameworks	Normalized Covariance Matrix	IterNorm	Notation
VICReg			VICReg
-	o		VICReg+NCM
-		o	VICReg+IterN
-	o	o	VbICReg

Table 7: Frameworks between VICReg and VbICReg: VICReg+NCM and VICReg+IterN.

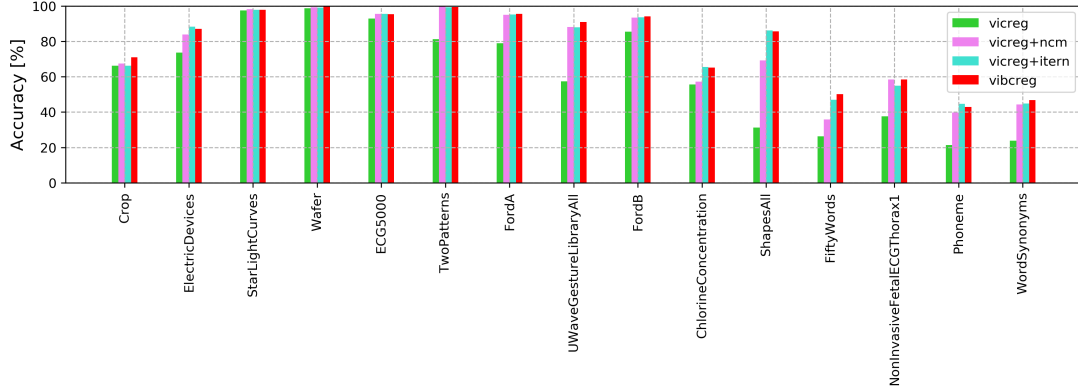


Figure 7: Comparative linear evaluation of the frameworks between VICReg and VIBCReg. It shows that either adding NCM (**ncm**) or IterNorm (**itern**) improves the performance. VIBCReg shows the most consistently-high performance among the four frameworks.

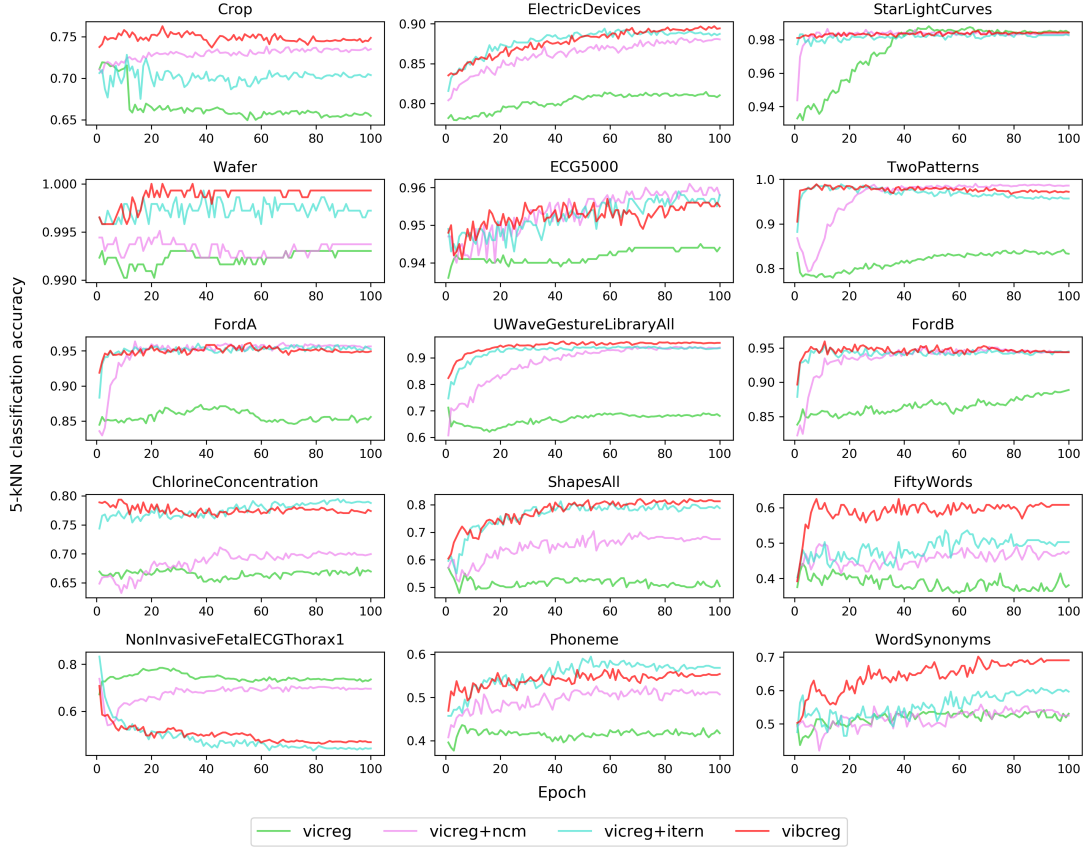


Figure 8: Comparative kNN accuracy of the frameworks between VICReg and VIBCReg. On most of the UCR datasets, VIBCReg and VICReg+IterN outperform the others, and VIBCReg shows the faster learning speed and the higher performance on several datasets than VICReg+IterN.



## 4.6 Sensitivity Test w.r.t Weight for the FD Loss

The normalized covariance matrix is proposed to alleviate an effort for tuning the weight hyperparameter  $\nu$  for the feature decorrelation loss term  $c(Z)$ . Without the normalization, a scale of  $c(Z)$  from the covariance matrix can be significantly large and wide, which would make the tuning process harder. To show that the tuning process is easier with the normalized covariance matrix (*i.e.*, performance is relatively quite consistent with respect to  $\nu$ ), sensitivity test results with respect to  $\nu$  are presented in Fig. 9.

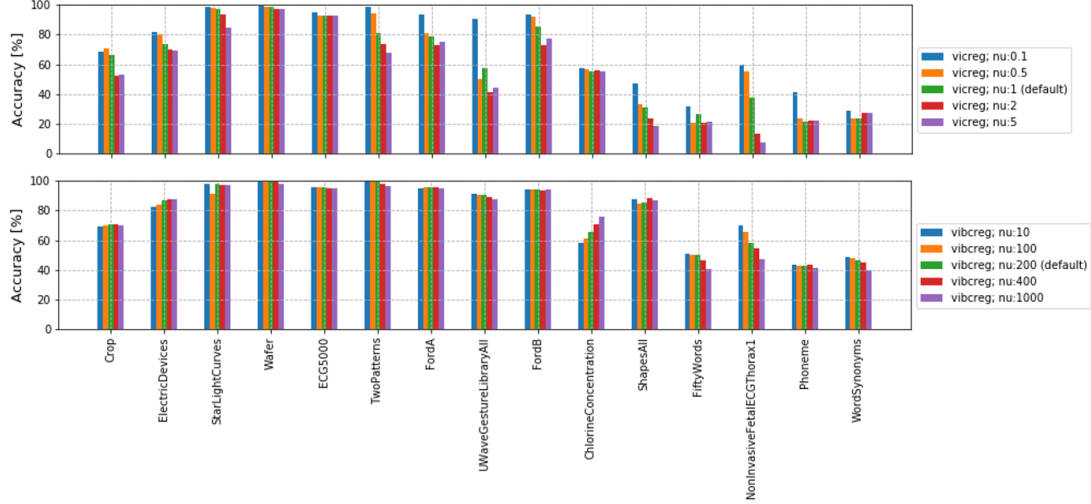


Figure 9: Linear evaluation of the sensitivity test with respect to  $\nu$ . Default values of  $\nu$  for VICReg and VIBCReg are 1 and 200, respectively. Variants of  $\nu$  are set by 5/10%, 50%, 200%, and 500% of the default values. It is apparent that the performance gaps between different  $\nu$  are much smaller for VIBCReg than VICReg in general, which makes the tuning process for  $\nu$  much easier.

## 5 Discussion

**Mean Shift (MSF) in VbIbCReg** VbIbCReg is proposed by adding the better invariance term on VIBCReg with MSF in an attempt to improve the performance even further. The idea of adding MSF itself is simple, but it comes with additional complexity introduced by the memory bank and the moving encoder. The memory bank and the moving encoder not only adds implementation complexity but also the GPU memory use and extra computational time. In the MSF paper [17], the authors state that the GPU memory is not an issue if the feature size is set to 512. However, the Barlow Twins paper [6] shows that use of the large feature size matters to maximize the performance, in which they increased the feature size of 16384 in their experiments. Then, a dilemma arises: using the large feature size is better, yet it would take too much GPU memory. Therefore, we settled on 4192 for our experiments. If VbIbCReg is used and one can experiment and find an optimal feature size given the trade-off.

**VbIbCReg vs. VIBCReg** Although we expected that VbIbCReg would perform better than VIBCReg since it has an advantage in optimizing the invariance term. Yet, VbIbCReg does not show any significant improvement over VbIbCReg. We suspect dataset size and a number of classes in a dataset. In the MSF paper, the framework is trained on ImageNet which has a large number of both samples and classes. However, in our experiments, the frameworks are trained on each of the relatively much smaller datasets. It may be possible that MSF reveals its advantage once trained on a large dataset with many classes. Therefore, experiments on a combined dataset of multiple datasets from the UCR archive will be conducted to see if MSF benefits the performance in our future study.

**Usability of VlbCReg** The most similar framework to VlbCReg is VICReg which was proposed in the computer vision domain. Despite its significant simplicity, it showed very competitive performances. VlbCReg is not so different from VICReg as VlbCReg is VICReg + IterNorm + normalized covariance matrix. Conceptually speaking, VlbCReg is VICReg with the better feature decorrelation. In that sense, there is no distinct/specific feature that is only subject to time series in VlbCReg. Hence, we are positive that VlbCReg would also be able to show competitive results in the computer vision domain.

## 6 Conclusion

In this paper we have introduced VlbCReg, which is an improved version of VICReg. By using a normalized covariance loss, we are able to improve the performance over all tested frameworks significantly for linear and fine-tuned time series classification. By using IterNorm in the last layer of the projector, we also reduce training for the model significantly.

While our application was on time series classification, we suspect that VlbCReg can improve on representation learning in computer vision as well.

## Acknowledgements

We would like to thank the Norwegian Research Council for funding the Machine Learning for Irregular Time Series (ML4ITS) project. This funding directly supported this research.

## References

- [1] Olivier J Hénaff, Ali Razavi, Carl Doersch, S. M. Ali Eslami, and Aaron Van Den Oord. Data-efficient image recognition with contrastive predictive coding. In *International Conference on Machine Learning*, 2019.
- [2] Ting Chen, Simon Kornblith, Mohammad Norouzi, and Geoffrey Hinton. A simple framework for contrastive learning of visual representations. In *International conference on machine learning*, pages 1597–1607. PMLR, 2020.
- [3] Kaiming He, Haoqi Fan, Yuxin Wu, Saining Xie, and Ross Girshick. Momentum contrast for unsupervised visual representation learning. In *Proceedings of the IEEE/CVF Conference on Computer Vision and Pattern Recognition*, pages 9729–9738, 2020.
- [4] Jean-Bastien Grill, Florian Strub, Florent Altché, Corentin Tallec, Pierre H Richemond, Elena Buchatskaya, Carl Doersch, Bernardo Avila Pires, Zhaohan Daniel Guo, Mohammad Gheshlaghi Azar, et al. Bootstrap your own latent: A new approach to self-supervised learning. *arXiv preprint arXiv:2006.07733*, 2020.
- [5] Xinlei Chen and Kaiming He. Exploring simple siamese representation learning, 2020.
- [6] Jure Zbontar, Li Jing, Ishan Misra, Yann Lecun, and Stéphane Deny. Barlow Twins: Self-Supervised Learning via Redundancy Reduction. In *arXiv*, 2021.
- [7] Adrien Bardes, Jean Ponce, and Yann LeCun. VICReg: Variance-Invariance-Covariance Regularization for Self-Supervised Learning. In *arXiv*, 2021.
- [8] Ting Chen, Simon Kornblith, Mohammad Norouzi, and Geoffrey Hinton. A simple framework for contrastive learning of visual representations, 2020.
- [9] Aleksandr Ermolov, Aliaksandr Siarohin, Enver Sangineto, and Nicu Sebe. Whitening for Self-Supervised Representation Learning, 2020.

- [10] Tianyu Hua, Wenxiao Wang, Zihui Xue, Yue Wang, Sucheng Ren, and Hang Zhao. On Feature Decorrelation in Self-Supervised Learning. In *arXiv*, 2021.
- [11] Lei Huang, Dawei Yang, Bo Lang, and Jia Deng. Decorrelated Batch Normalization. In *Proceedings of the IEEE Computer Society Conference on Computer Vision and Pattern Recognition*, pages 791–800, 2018.
- [12] Spyros Makridakis, Evangelos Spiliotis, and Vassilios Assimakopoulos. The m4 competition: Results, findings, conclusion and way forward. *International Journal of Forecasting*, 34(4):802–808, 2018.
- [13] S Makridakis, E Spiliotis, and V Assimakopoulos. The m5 accuracy competition: Results, findings and conclusions. *International Journal of Forecasting*, 2020.
- [14] Yanping Chen, Eamonn Keogh, Bing Hu, Nurjahan Begum, Anthony Bagnall, Abdullah Mueen, and Gustavo Batista. The ucr time series classification archive, July 2015.
- [15] Erick A Perez Alday, Annie Gu, Amit J Shah, Chad Robichaux, An Kwok Ian Wong, Chengyu Liu, Feifei Liu, Ali Bahrami Rad, Andoni Elola, Salman Seyed, Qiao Li, Ashish Sharma, Gari D Clifford, and Matthew A Reyna. Classification of 12-lead ECGs: The PhysioNet/Computing in Cardiology Challenge 2020. *Physiological Measurement*, 41(12):124003, 2020.
- [16] Patrick Wagner, Nils Strodthoff, Ralf Dieter Boussejot, Dieter Kreiseler, Fatima I. Lunze, Wojciech Samek, and Tobias Schaeffter. PTB-XL, a large publicly available electrocardiography dataset. *Scientific Data*, 7(1):1–15, 12 2020.
- [17] Soroush Abbasi Koohpayegani, Ajinkya Tejankar, and Hamed Pirsiavash. Mean Shift for Self-Supervised Learning. In *arXiv*, 2021.
- [18] Temesgen Mehari and Nils Strodthoff. Self-supervised representation learning from 12-lead ECG data. *arXiv*, 3 2021.
- [19] Mathilde Caron, Priya Goyal, Ishan Misra, Piotr Bojanowski, Julien Mairal, and Armand Joulin. Unsupervised Learning of Visual Features by Contrasting Cluster Assignments, 2020.
- [20] Gregory Koch, Richard Zemel, and Ruslan Salakhutdinov. Siamese Neural Networks for One-Shot Image Recognition. In *ICML - Deep Learning Workshop*, volume 7, pages 956–963, 2015.
- [21] Sumit Chopra, Raia Hadsell, and Yann LeCun. Learning a similarity metric discriminatively, with application to face verification. In *Proceedings - 2005 IEEE Computer Society Conference on Computer Vision and Pattern Recognition, CVPR 2005*, volume I, pages 539–546, 2005.
- [22] Aaron Van Den Oord, Yazhe Li, and Oriol Vinyals. Representation learning with contrastive predictive coding, 2018.
- [23] Kaiming He, Xiangyu Zhang, Shaoqing Ren, and Jian Sun. Deep residual learning for image recognition. In *Proceedings of the IEEE Computer Society Conference on Computer Vision and Pattern Recognition*, volume 2016-Decem, pages 770–778, 2016.
- [24] Junyoung Chung, Caglar Gulcehre, KyungHyun Cho, and Yoshua Bengio. Empirical Evaluation of Gated Recurrent Neural Networks on Sequence Modeling. In *arXiv*, 12 2014.
- [25] Zhirong Wu, Yuanjun Xiong, Stella X. Yu, and Dahua Lin. Unsupervised Feature Learning via Non-parametric Instance Discrimination. In *Proceedings of the IEEE Computer Society Conference on Computer Vision and Pattern Recognition*, pages 3733–3742. IEEE Computer Society, 12 2018.

- [26] Dariusz Dereniowski and Marek Kubale. Cholesky factorization of matrices in parallel and ranking of graphs. In *International Conference on Parallel Processing and Applied Mathematics*, volume 3019, pages 985–992. Springer Verlag, 2003.
- [27] Aliaksandr Siarohin, Enver Sangineto, and Nicu Sebe. Whitening and coloring batch transform for GANS. In *7th International Conference on Learning Representations, ICLR 2019*, 2019.
- [28] Lei Huang, Yi Zhou, Fan Zhu, Li Liu, and Ling Shao. Iterative normalization: Beyond standardization towards efficient whitening. In *Proceedings of the IEEE Computer Society Conference on Computer Vision and Pattern Recognition*, volume 2019-June, pages 4869–4878, 2019.
- [29] Ilya Loshchilov and Frank Hutter. Decoupled weight decay regularization. In *7th International Conference on Learning Representations, ICLR 2019*, 2019.
- [30] Ilya Loshchilov and Frank Hutter. SGDR: Stochastic gradient descent with warm restarts. In *5th International Conference on Learning Representations, ICLR 2017 - Conference Track Proceedings*, 2017.
- [31] Adam Paszke, Sam Gross, Francisco Massa, Adam Lerer, James Bradbury, Gregory Chanan, Trevor Killeen, Zeming Lin, Natalia Gimelshein, Luca Antiga, Alban Desmaison, Andreas Kopf, Edward Yang, Zachary DeVito, Martin Raison, Alykhan Tejani, Sasank Chilamkurthy, Benoit Steiner, Lu Fang, Junjie Bai, and Soumith Chintala. Pytorch: An imperative style, high-performance deep learning library. In H. Wallach, H. Larochelle, A. Beygelzimer, F. d'Alché-Buc, E. Fox, and R. Garnett, editors, *Advances in Neural Information Processing Systems 32*, pages 8024–8035. Curran Associates, Inc., 2019.
- [32] Fei Wang. Multi-Scale-1D-ResNet. <https://github.com/geekfeiw/Multi-Scale-1D-ResNet>, 2018.
- [33] S. Ioffe and C. Szegedy. Batch normalization: Accelerating deep network training by reducing internal covariate shift. In *32nd International Conference on Machine Learning, ICML 2015*, volume 1, pages 448–456. International Machine Learning Society (IMLS), 2015.
- [34] Nils Strodthoff, Patrick Wagner, Tobias Schaeffter, and Wojciech Samek. Deep learning for ECG analysis: Benchmarks and insights from PTB-XL, 2020.
- [35] F. Pedregosa, G. Varoquaux, A. Gramfort, V. Michel, B. Thirion, O. Grisel, M. Blondel, P. Prettenhofer, R. Weiss, V. Dubourg, J. Vanderplas, A. Passos, D. Cournapeau, M. Brucher, M. Perrot, and E. Duchesnay. Scikit-learn: Machine learning in Python. *Journal of Machine Learning Research*, 12:2825–2830, 2011.

## A Pseudocode for VlbCReg

---

**Algorithm 1** PyTorch-style pseudocode for VlbCReg

---

```

1 # f: encoder network
2 # lambda_, mu, nu: coefficients of the invariance, variance, and covariance
3 # losses
4 # N: batch size
5 # F: feature size (= dimension of the representations)
6 #
7 # mse_loss: Mean square error loss function
8 # off_diagonal: off-diagonal elements of a matrix
9 # relu: ReLU activation function
10 # normalize: torch.nn.functional.normalize(..)
11
12 for x in loader: # load a batch with N samples
13     # two randomly augmented versions of x
14     x_a, x_b = augment(x)
15
16     # compute representations
17     z_a = f(x_a) # N x F
18     z_b = f(x_b) # N x F
19
20     # invariance loss
21     sim_loss = mse_loss(z_a, z_b)
22
23     # variance loss
24     std_z_a = torch.sqrt(z_a.var(dim=0) + 1e-4)
25     std_z_b = torch.sqrt(z_b.var(dim=0) + 1e-4)
26     std_loss = torch.mean(relu(1 - std_z_a))
27     std_loss = std_loss + torch.mean(relu(1 - std_z_b))
28
29     # covariance loss
30     z_a = z_a - z_a.mean(dim=0)
31     z_b = z_b - z_b.mean(dim=0)
32     norm_z_a = normalize(z_a, p=2, dim=0)
33     norm_z_b = normalize(z_b, p=2, dim=0)
34     norm_cov_z_a = (norm_z_a.T @ norm_z_a)
35     norm_cov_z_b = (norm_z_b.T @ norm_z_b)
36     norm_cov_loss = (off_diagonal(norm_cov_z_a)**2).mean() \
37         + (off_diagonal(norm_cov_z_b)**2).mean()
38
39     # loss
40     loss = lambda_ * sim_loss + mu * std_loss + nu * norm_cov_loss
41
42     # optimization step
43     loss.backward()
44     optimizer.step()

```

---

Table 8: Pseudocode for VlbCReg. We mostly follow the same notations from the VICReg paper.

## B Architecture of VbIbCReg

The original implementation of MSF consists of a backbone (*i.e.*, ResNet), projector, and predictor. Its projector is arranged as follows: (Linear(4096)-BN-ReLU)-(Linear(512)) and its predictor is: (Linear(4096)-BN-ReLU)-(Linear(512)), where the values in the parenthesis denotes the hidden layer size of a linear layer. Comparing it with VlbCReg, the main difference lies in the use of the predictor. In our experiments as shown in Table 9, the presence of the predictor does not provide much performance improvement, therefore, the predictor is not used. In the experiments, the predictor is implemented as in the MSF paper. Hence, the output from the backbone-projector is treated as *query*. It should be noted that the projector in VbIbCReg is the same as the VlbCReg’s projector.

Dataset name	w/o predictor	with predictor
Crop	72.3	<b>73.1</b>
ElectricDevices	84.8	<b>86.2</b>
StarLightCurves	<b>98.1</b>	97.7
Wafer	<b>99.5</b>	<b>99.5</b>
ECG5000	<b>95.3</b>	<b>95.3</b>
TwoPatterns	<b>99.3</b>	<b>99.3</b>
FordA	<b>95.4</b>	95.3
UWaveGestureLibraryAll	<b>90.3</b>	90.2
FordB	<b>93.9</b>	93.8
ChlorineConcentration	63.6	<b>66.6</b>
ShapesAll	<b>86.7</b>	85.8
FiftyWords	<b>0.5083</b>	50.3
NonInvasiveFetalECGThorax1	<b>72.5</b>	63.6
Phoneme	41.2	<b>43.6</b>
WordSynonyms	<b>49.2</b>	48.1

Table 9: Linear evaluation with respect to the use of the predictor for VbIbCReg. The values in the table denote the accuracy. The evaluation was conducted on one random seed.

## C Data Augmentation Methods

### C.1 Methods

In our experiments, three data augmentation methods are used: **Random Crop**, **Random Amplitude Resize**, and **Random Vertical Shift**.

**Random Crop** is similar to the one in computer vision. The only difference is that the random crop is conducted on 1D time series data in our experiments. Its hyperparameter is crop size. The crop size is set to a half length of input time series for most of the UCR datasets. A summary of the crop size for each UCR dataset is presented in Table 10. Note that the crop size for PTB-XL is 2.5s as previously suggested in [18].

**Random Amplitude Resize** randomly resizes overall amplitude of input time series. It is expressed as Eq. (10), where  $m_{\text{rar}}$  is a multiplier to input time series  $x$ , and  $\alpha_{\text{rar}}$  is a hyperparameter. In our experiments,  $\alpha_{\text{rar}}$  is set to 0.3 unless specified differently.

$$x = m_{\text{rar}} x; \quad m_{\text{rar}} \sim \text{U}(1 - \alpha_{\text{rar}}, 1 + \alpha_{\text{rar}}) \quad (10)$$

**Random Vertical Shift** randomly shifts input time series in a vertical direction. It is expressed as Eq. (11), where  $x'$  denotes input time series before any augmentation,  $\text{Std}$  denotes a standard deviation estimator, and  $\beta_{\text{rvs}}$  is a hyperparameter to determine a magnitude of the vertical shift. In our experiments,  $\beta_{\text{rvs}}$  is set to 0.5 unless specified differently.

$$x = x + s_{\text{rvs}}; \quad s_{\text{rvs}} \sim \text{U}(-\alpha_{\text{rvs}}, \alpha_{\text{rvs}}) \quad (11)$$

$$\alpha_{\text{rvs}} = \beta_{\text{rvs}} \text{Std}(x') \quad (12)$$

Dataset name	Length	Use half length for crop	Crop size
Crop	46	x	46
ElectricDevices	96	o	48
StarLightCurves	1024	o	512
Wafer	152	x	152
ECG5000	140	o	70
TwoPatterns	128	o	64
FordA	500	o	250
UWaveGestureLibraryAll	945	o	473
FordB	500	o	250
ChlorineConcentration	166	x	166
ShapesAll	512	o	256
FiftyWords	270	o	135
NonInvasiveFetalECGThorax1	750	x	750
Phoneme	1024	o	512
WordSynonyms	270	o	135

Table 10: Summary of the crop size for each UCR dataset.

## D Encoder

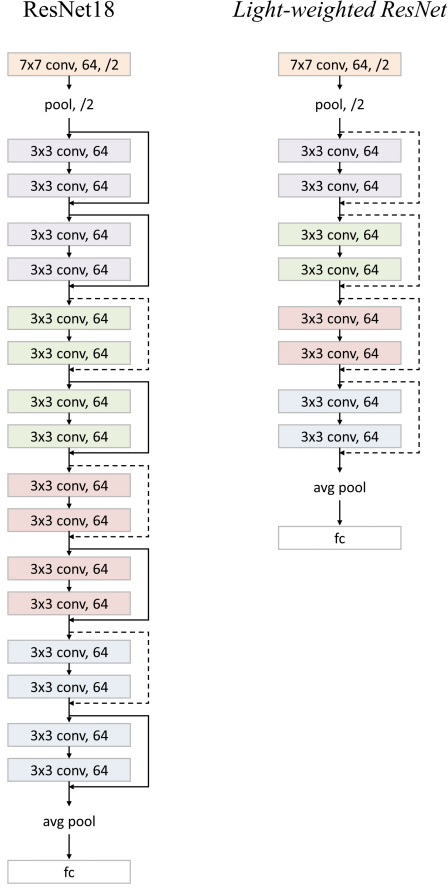


Figure 10: The light-weighted ResNet is illustrated compared to ResNet18.

The light-weighted ResNet presented in Fig. 10 is used in our experiments. The illustration is in the same format as in the original ResNet paper [23].

## E FD and FcE Metrics

FD and FcE metrics are metrics for the feature decorrelation and feature component expressiveness. They are used to keep track of FD and FcE status of learned features during SSL for representation learning. The FD metrics and FcE metrics are defined in Eq. (14) and Eq. (15), respectively.  $Z$  is output from the projector and  $F$  is feature size of  $Z$ .  $\sum_{i \neq j}$  denotes ignoring the diagonal terms in the matrix. In Eq. (13), the l2-norm is conducted along the batch dimension. In Eq. (15), Std denotes a standard deviation estimator and it is conducted along the batch dimension.

$$C(Z) = \left( \frac{Z - \bar{Z}}{\|Z - \bar{Z}\|_2} \right)^T \left( \frac{Z - \bar{Z}}{\|Z - \bar{Z}\|_2} \right) \quad (13)$$

$$\mathcal{M}_{\text{FD}} = \frac{1}{F^2} \sum_{i \neq j} |C(Z)| \quad (14)$$



$$\mathcal{M}_{\text{FcE}} = \frac{1}{F} \sum_{f=1}^F \text{Std}(Z) \quad (15)$$

## F Additional Materials for Some Sections

### F.1 Faster Representation Learning by VibCReg

The FD and FcE metrics that correspond to Fig. 4 (*i.e.*, 5-kNN classification accuracy on the UCR datasets) are presented in Figs. 11-12, respectively. The FD and FcE metrics that correspond to Fig. 5 (*i.e.*, kNN macro F1 score on the PTB-XL dataset during the representation learning) are presented in Fig.13.

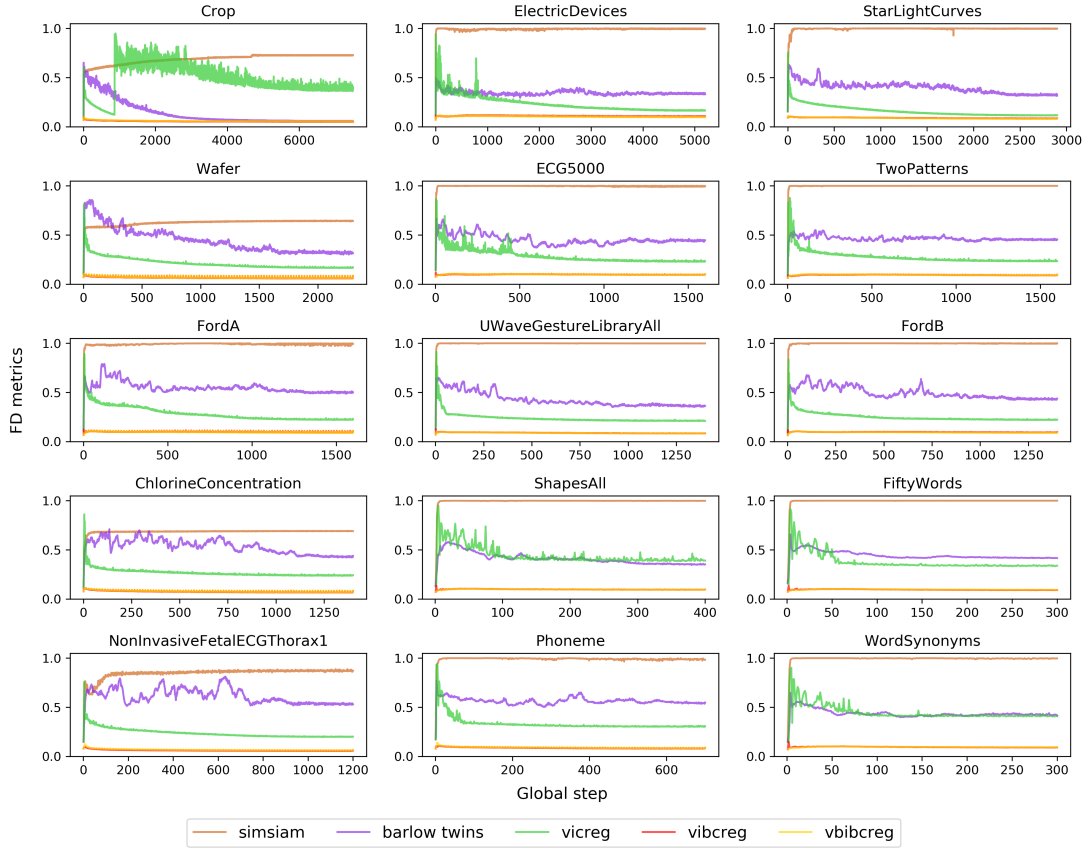


Figure 11: FD metrics on the UCR datasets during the representation learning. It is noticeable that the metrics of VibCReg and VbIBCReg converge to near-zero in the beginning, ensuring the feature decorrelation throughout the entire training epochs.

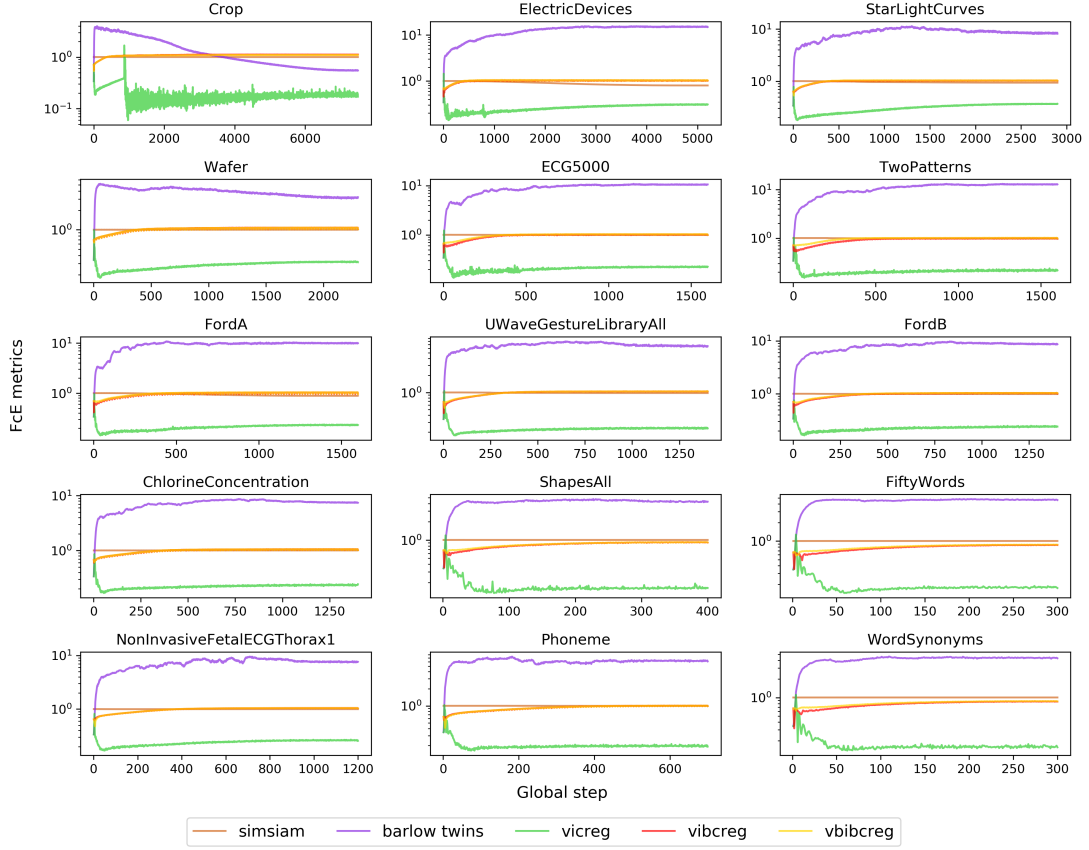


Figure 12: FcE metrics on the UCR datasets during the representation learning. Note that y-axis is log-scaled. It can be observed that metrics of VIBCReg and VbIBCReg converges to 1 fairly quickly, ensuring the feature component expressiveness throughout the entire training epochs.

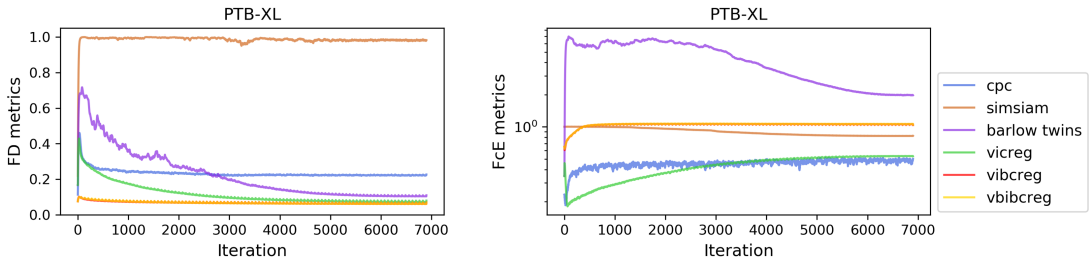


Figure 13: FD and FcE metrics on the PTB-XL during the representation learning. Similar to the FD and FcE metrics on the UCR datasets, VIBCReg and VbIBCReg show the fastest convergence to the optimal values. An exponential moving average with the window size of 10 is applied to the results here.

## F.2 Between VICReg and VIBCReg

FD metrics and FcE metrics that correspond to Fig. 8 (*i.e.*, Comparative kNN accuracy of the frameworks between VICReg and VIBCReg) are presented in Fig. 14 and Fig. 15, respectively.

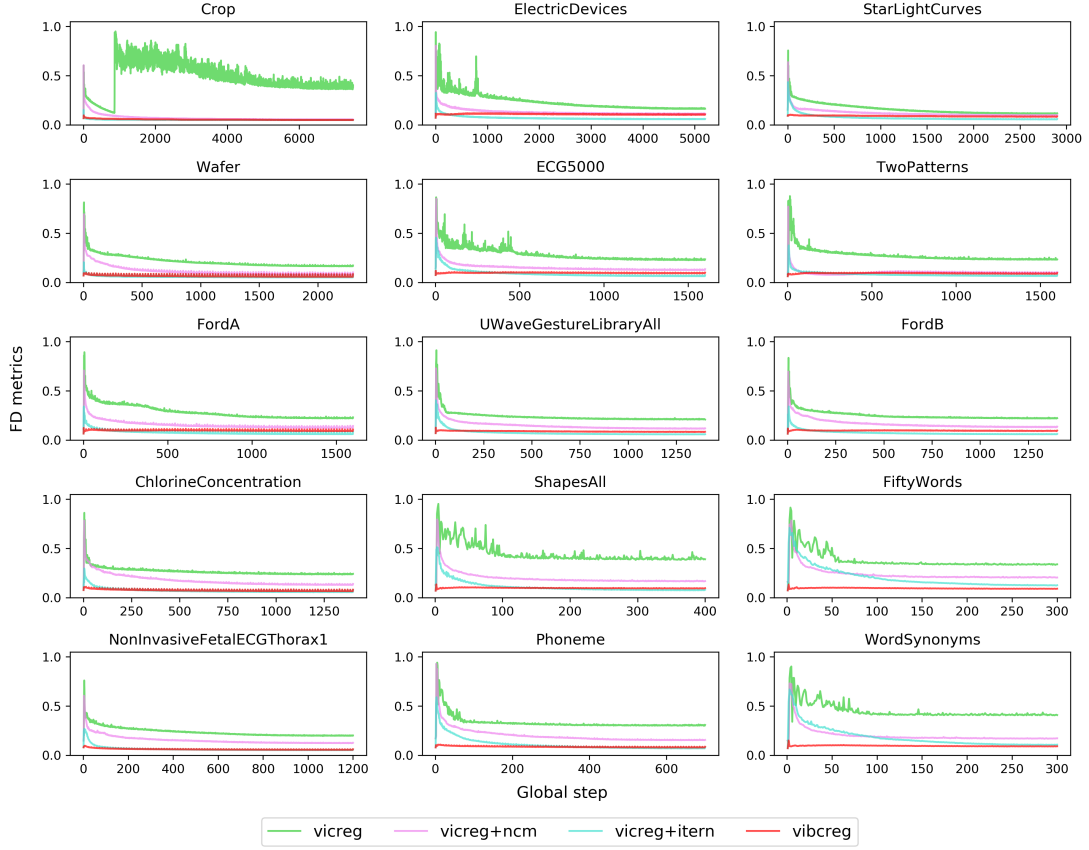


Figure 14: FD metrics of the frameworks between VICReg and VibCReg on the UCR datasets. **ncm** and **itern** denote the normalized covariance matrix and IterNorm, respectively. It can be seen that VibCReg shows the fastest convergence with the lowest FD metrics on most of the datasets. Both NCM and IterN seem to improve the feature decorrelation while IterN brings the higher feature decorrelation. Use both NCM and IterN leads to the highest feature decorrelation. Note that VibCReg is VICReg+NCM+IterN.

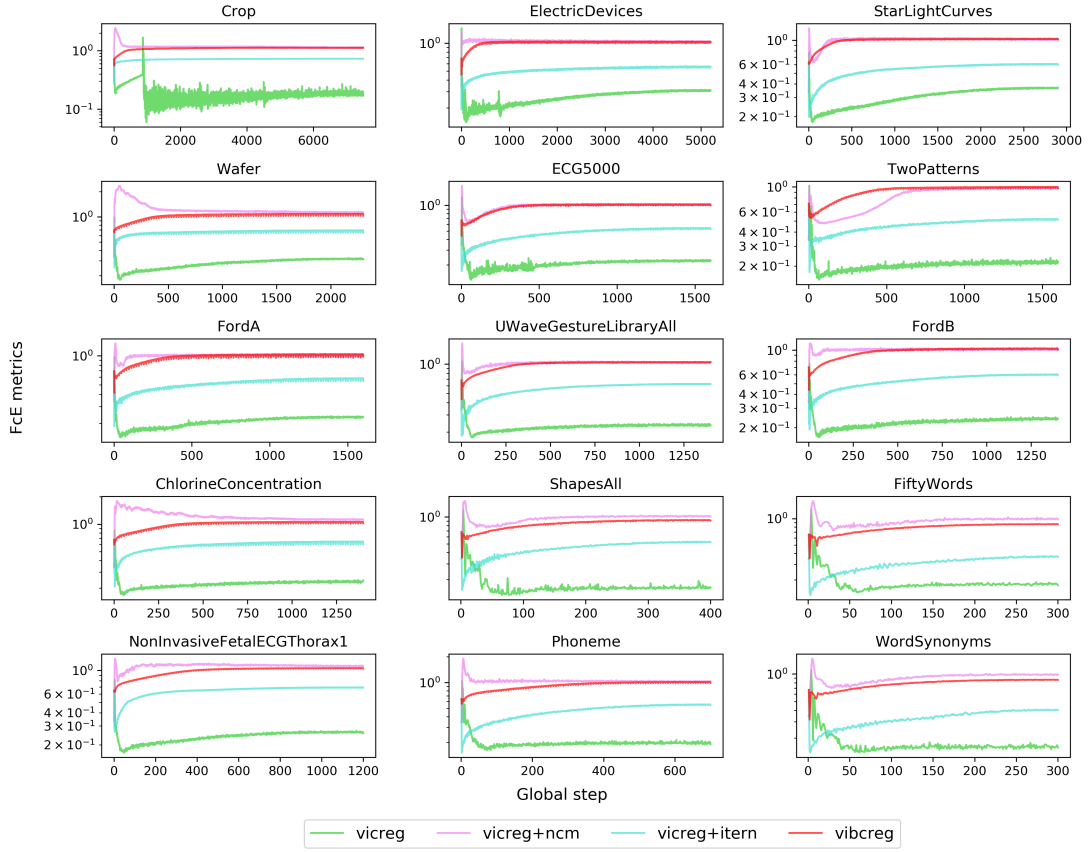


Figure 15: FcE metrics of the frameworks between VICReg and ViBCReg on the UCR datasets. **ncm** and **itern** denote the normalized covariance matrix and IterNorm, respectively. It can be observed that the use of NCM results in the faster convergence of the feature component expressiveness.